Electromagnetic velocity fields near a conducting slab

W. L. Schaich
Physics Department, Indiana University, Bloomington, Indiana 47405
(Received 21 December 2000; published 21 September 2001)

A calculational scheme for the electromagnetic fields of a charge moving at constant velocity parallel to a flat conducting slab is developed. The results can be evaluated for arbitrary speed of the charge. Comparisons are made with earlier work that was mostly limited to a low-speed approximation. Both analytic insights and numerical illustrations of the theory are given.

DOI: 10.1103/PhysRevE.64.046605 PACS number(s): 03.50.De, 41.20.Gz

I. INTRODUCTION

In this paper we develop a complete solution for a (deceptively) simple question in electromagnetism. One imagines a charge e moving at constant speed v outside the flat face of a conducting slab of thickness d. The problem is to determine the $\vec{E}$ and $\vec{B}$ fields associated with this steady motion, both inside and outside the conductor. This question has attracted several efforts over the last 30 years and some controversy; see the literature survey in Ref. [1]. Most authors have used a perturbative approach in which the speed is assumed to be suitably small. Only in the paper by Jones [2] is this ''low-speed'' approximation not made, but he treats a line of charge moving perpendicular to its length (and parallel to the conductor's surface), not a point charge.

Here we show how to solve the problem for a point charge moving at arbitrary (but constant) speed. The fields are expanded in a Fourier series based on two-dimensional wave vectors lying in the plane of the surface. Although numerical integration is needed for a general evaluation of the fields, the Fourier representation is compact and allows considerable insight by analogies that one can make with the well known calculation of reflection and transmission of a light beam by a slab.

In Sec. II we present our derivation and examine various limiting cases: $d\to\infty$, $d\to 0$, $v\to 0$, and the conductivity σ becoming nil or infinite. These allow us to make contact with earlier work. We also consider various linear superpositions of our results, in order to treat drifting lines of charge moving either perpendicular or parallel to their length. For the latter case, one has in effect a dc current in a fixed wire parallel to the conductor. From our general solution we find then, as expected, that the associated magnetic field is completely unaffected by the conductor (as long as its dc conductivity is not infinite).

In Sec. III several model calculations are described. These compare for the magnetic field the unscreened form, the low-speed answer, and our new general results for different choices of v, d, and σ. In particular we show when and how the low-speed answer fails as v increases.

II. DERIVATION

Begin with the simpler situation of a charge moving through a homogeneous dielectric. The prescribed trajectory of constant velocity can be described by the charge and current densities:

$$\rho(\vec{x},t)=e\,\delta(x-h)\,\delta(y-vt)\,\delta(z), \tag{1}$$

$$\vec{j}(\vec{x},t)=v\hat{y}\rho(\vec{x},t), \tag{2}$$

with both $h>0$ and $v>0$ independent of time, t. The conducting slab, which is not yet present, will be placed between $x=0$ and $x=-d<0$ and will fill the y-z plane. The Fourier transforms of ρ and $\vec{j}$ are

$$\rho(\vec{q},\omega)=\int dt\, e^{i\omega t}\int d^3x\, e^{-i\vec{q}\cdot\vec{x}}\rho(\vec{x},t)$$

$$=2\pi e\,\delta(\omega-\vec{q}\cdot\vec{v})e^{-iq_x h} \tag{3}$$

$$\vec{j}(\vec{q},\omega)=\vec{v}\rho(\vec{q},\omega), \tag{4}$$

where $\vec{v}=v\hat{y}$. From these one can readily determine the scalar and vector potentials in the Lorentz gauge [3],

$$\left.\begin{matrix}\Phi(\vec{q},\omega)\\ \vec{A}(\vec{q},\omega)\end{matrix}\right\}=\frac{4\pi}{|\vec{q}|^2-\dfrac{\omega^2}{c^2}\varepsilon}\times\begin{cases}\rho(\vec{q},\omega)/\varepsilon\\ \vec{j}(\vec{q},\omega)/c,\end{cases} \tag{5}$$

with c the vacuum speed of light, and from them the fields $\vec{E}=-i\vec{q}\Phi+(i\omega/c)\vec{A}$ and $\vec{B}=i\vec{q}\times\vec{A}$.

Finally we would like to transform back to real space. For the electric field this leads to

$$\vec{E}(\vec{x},t)=-i\int\frac{d^3q}{(2\pi)^3}$$

$$\times\frac{4\pi e/\varepsilon}{|\vec{q}|^2-\dfrac{\omega^2}{c^2}\varepsilon}e^{iq_x(x-h)}e^{iq_y(y-vt)}e^{iq_z z}$$

$$\times(q_x,q_y(1-\beta^2\varepsilon),q_z), \tag{6}$$

where $\beta=v/c$ and the triplet of symbols at the end of the integrand describe the x, y, and z components. To proceed, we now assume for simplicity that ε is a real-valued constant, independent of both $\vec{q}$ and $\omega=\vec{q}\cdot\vec{v}$, and that the speed is too slow for Cerenkov radiation, so $1-\beta^2\varepsilon>0$. Introduce $\gamma'=1/\sqrt{1-\beta^2\varepsilon}$ and change integration variables to $\vec{q}'$ where $q_x'=q_x$, $q_y'=q_y/\gamma'$, $q_z'=q_z$. Then

$$\varepsilon\vec{E}(\vec{x},t)=-\gamma'\left(\frac{\partial}{\partial x},\frac{1}{\gamma'^2}\frac{\partial}{\partial y},\frac{\partial}{\partial z}\right)\times\int\frac{d^3q'}{(2\pi)^3}\frac{4\pi e}{|\vec{q}'|^2}e^{iq'_x(x-h)}\times\exp[iq'_y\gamma'(y-vt)]e^{iq'_z z}=\frac{\gamma' e(x-h,y-vt,z)}{[(x-h)^2+\gamma'^2(y-vt)^2+z^2]^{3/2}}. \tag{7}$$

The calculation of $\vec{B}$ may be done similarly to yield

$$\vec{B}(\vec{x},t)=\vec{\beta}\times\varepsilon\vec{E}(\vec{x},t). \tag{8}$$

We have reproduced these well known [3] results for the velocity fields of an isolated single charge to assure the reader that the Fourier space approach can retain all relativistic effects.

In order to apply this approach when a conducting slab is present, we need to rewrite and reinterpret the above equations. In Eq. (6) the integral over q_x can be done for ε an arbitrary [4], complex-valued function of $\omega=q_y v$ to yield

$$D(\vec{x},t)=-i\int\frac{d^2Q}{(2\pi)^2}\frac{2\pi e}{\overline{Q}}e^{iQ_y(y-vt)}e^{iQ_z z}(i\overline{Q}\,\mathrm{sgn}(x-h),\ Q_y(1-\beta^2\varepsilon),Q_z)e^{-\overline{Q}|x-h|}, \tag{9}$$

where $\vec{D}=\varepsilon\vec{E}$ is the displacement field and we have changed from (q_y,q_z) to (Q_y,Q_z), which are the components of the two-dimensional vector $\mathbf{Q}$ in the y-z plane. The quantity $\overline{Q}$ is determined by

$$\overline{Q}^2=Q_y^2(1-\beta^2\varepsilon)+Q_z^2=|\mathbf{Q}|^2-\frac{\omega^2}{c^2}\varepsilon(\omega), \tag{10}$$

and $\overline{Q}$ is to be chosen with positive real part [4]. For $0<x<h$ we can then rewrite Eq. (9) as

$$\vec{D}(\vec{x},t)=\int\frac{d^2Q}{(2\pi)^2}\vec{D}_{\mathrm{inc}}(x;\mathbf{Q},\omega)\exp[i(Q_y y+Q_z z-\omega t)], \tag{11}$$

where $\omega=Q_y v$ and

$$\vec{D}_{\mathrm{inc}}(x;\mathbf{Q},\omega)=\left(\frac{2\pi e}{\overline{Q}}e^{-\overline{Q}h}\right)\times e^{+\overline{Q}x}(-\overline{Q},-iQ_y(1-\beta^2\varepsilon),-iQ_z). \tag{12}$$

When the conducting slab is in place we interpret Eqs. (11) and (12) as representing a sum of transverse, electromagnetic partial waves incident on the slab. These waves will be reflected by and transmitted into and through the slab. The multiple scattering process can be described independently for each $\mathbf{Q}$ and ω.

We can further simplify the calculation if we separate the polarization in Eq. (12) into s- and p-wave parts. To this end introduce

$$\vec{\varepsilon}^{(p)}_{\pm}(\mathbf{Q})=\left(\mp1,-\frac{i\overline{Q}}{Q^2}Q_y,-i\frac{\overline{Q}}{Q^2}Q_z\right), \tag{13}$$

$$\vec{\varepsilon}^{(s)}_{\pm}(\mathbf{Q})=\left(0,\frac{iQ_z}{\overline{Q}}\varepsilon,\frac{-iQ_y}{\overline{Q}}\varepsilon\right). \tag{14}$$

One can readily check that each of these is orthogonal to the ''wave vector,'' $i\vec{q}_{\pm}=(\pm\overline{Q},iQ_y,iQ_z)$, associated with $e^{\pm\overline{Q}x}e^{iQ_y y}e^{iQ_z z}$. Further $\vec{\varepsilon}^{(p)}$ lies in the plane of incidence (defined by $\hat{x}$ and $\mathbf{Q}$) while $\vec{\varepsilon}^{(s)}$ is perpendicular to it. Using them as basis vectors for the polarization we have

$$[\mp\overline{Q},-iQ_y(1-\beta^2\varepsilon),-iQ_z]/\overline{Q}=e_p\vec{\varepsilon}^{(p)}_{\pm}+e_s\vec{\varepsilon}^{(s)}_{\pm}, \tag{15}$$

where

$$e_p=1,\quad e_s=\beta^2\frac{Q_y Q_z}{Q^2}. \tag{16}$$

We have chosen the definitions of the $\vec{\varepsilon}_{\pm}$'s so that the e's are real, dimensionless, and independent of medium. With the decomposition (15) one can use the optics analogy to be sure that there will be no mixing of these polarizations through the multiple scattering process.

The full calculation of the velocity field has now been reduced to a standard problem in optics [5]. We use a matching procedure to solve it. There are three media. For $x>0$ we have vacuum with $\varepsilon_1=1$. For $-d<x<0$, there is the conductor with ε_2, which we do not need to describe further yet [4], except that ε_2 depends only on $\omega=Q_y v$ so one can use classical (local) optics. For $x<-d$, we are back to vacuum with $\varepsilon_3=\varepsilon_1=1$. Then Eq. (11) is generalized to

$$\vec{D}(\vec{x},t)=\int\frac{d^2Q}{(2\pi)^2}\vec{D}_{\mathrm{total}}(x;\mathbf{Q},\omega=Q_y v)e^{iQ_y(y-vt)}e^{iQ_z z}, \tag{17}$$

with $\vec{D}_{\mathrm{total}}/(2\pi e\,e^{-\overline{Q}_1 h})$ given in the three regions $0<x<h$, $-d<x<0$, $x<-d$, respectively, by

$$e_p[\vec{\varepsilon}^{(p)}_{+,1}e^{\overline{Q}_1 x}+r_p\vec{\varepsilon}^{(p)}_{-,1}e^{-\overline{Q}_1 x}]+e_s[\vec{\varepsilon}^{(s)}_{+,1}e^{\overline{Q}_1 x}+r_s\vec{\varepsilon}^{(s)}_{-,1}e^{-\overline{Q}_1 x}], \tag{18a}$$

$$e_p[\alpha^{(p)}_{+}\vec{\varepsilon}^{(p)}_{+,2}e^{\overline{Q}_2 x}+\alpha^{(p)}_{-}\vec{\varepsilon}^{(p)}_{-,2}e^{-\overline{Q}_2(x+d)}]+e_s[\alpha^{(s)}_{+}\vec{\varepsilon}^{(s)}_{+,2}e^{\overline{Q}_2 x}+\alpha^{(s)}_{-}\vec{\varepsilon}^{(s)}_{-,2}e^{-\overline{Q}_2(x+d)}], \tag{18b}$$

$$e_p t_p\varepsilon^{(p)}_{+,3}e^{\overline{Q}_3(x+d)}+e_s t_s\vec{\varepsilon}^{(s)}_{+,3}e^{\overline{Q}_3(x+d)}. \tag{18c}$$

Before matching these partial waves across $x=0$ and $x=-d$ to determine the r's, t's, and α's, we write out the corresponding magnetic field, which follows from Faraday's law: $i(\omega/c)\varepsilon\vec{B}=i\vec{q}\times\vec{D}$. Since $\vec{q}\times\vec{\varepsilon}^{(p)}\propto\vec{\varepsilon}^{(s)}$ and vice versa, we readily find

$$\vec{B}(\vec{x},t)=\int\frac{d^2Q}{(2\pi)^2}\vec{B}_{\text{total}}(x;\mathbf{Q},\omega=Q_y v)e^{iQ_y(y-vt)}e^{iQ_z z}, \tag{19}$$

with $\vec{B}_{\text{total}}/(2\pi e\beta i e^{-\overline{Q}_1 h})$ given in the three regions $0<x<h$, $-d<x<0$, $x<-d$, respectively, by

$$b_p\frac{\overline{Q}_1}{Q\varepsilon_1}[\vec{\varepsilon}^{(s)}_{+,1}e^{\overline{Q}_1 x}-r_p\vec{\varepsilon}^{(s)}_{-,1}e^{-\overline{Q}_1 x}]+b_s\frac{Q_z}{\overline{Q}_1}[\vec{\varepsilon}^{(p)}_{+,1}e^{\overline{Q}_1 x}-r_s\vec{\varepsilon}^{-\overline{Q}_1 x}_{-,1}], \tag{20a}$$

$$b_p\frac{\overline{Q}_2}{Q\varepsilon_2}[\alpha^{(p)}_{+}\vec{\varepsilon}^{(s)}_{+,2}e^{\overline{Q}_2 x}-\alpha^{(p)}_{-}\vec{\varepsilon}^{(s)}_{-,2}e^{-\overline{Q}_2(x+d)}]+b_s\frac{Q_z}{\overline{Q}_2}[\alpha^{(s)}_{+}\vec{\varepsilon}^{(p)}_{+,2}-\alpha^{(s)}_{-}\vec{\varepsilon}^{(p)}_{+,2}e^{\overline{Q}_2(x+d)}], \tag{20b}$$

$$b_p\frac{\overline{Q}_3}{Q\varepsilon_3}t_p\vec{\varepsilon}^{(s)}_{+,3}e^{\overline{Q}_3(x+d)}+b_s\frac{Q_z}{\overline{Q}_3}t_s\vec{\varepsilon}^{(p)}_{+,3}e^{\overline{Q}_3(x+d)}, \tag{20c}$$

where

$$b_p=Q_y/Q,\quad b_s=1. \tag{21}$$

For the matching process we require continuity for the normal components of $\vec{D}$ and $\vec{B}$ and for the parallel components of $\vec{E}=\vec{D}/\varepsilon$ and $\vec{H}=\vec{B}$. Several of these matching equations are redundant and we end up with just enough to solve for the unknowns. The normalizations in Eqs. (18) and (20) have been chosen so that the forms of the solutions are the same for s and p waves. We find (when $\varepsilon_3=\varepsilon_1$)

$$\alpha_-=\mathfrak{r}e^{-\overline{Q}_2 d}\alpha_+,\quad t=\mathfrak{t}e^{-\overline{Q}_2 d}\alpha_+,$$
$$\alpha_+=\frac{2/(1+\Gamma)}{1-\mathfrak{r}^2e^{-2\overline{Q}_2 d}},\quad r=-\mathfrak{r}\frac{(1-e^{-2\overline{Q}d})}{(1-\mathfrak{r}^2e^{-2\overline{Q}d})}, \tag{22}$$

where $\mathfrak{r}=(1-\Gamma)/(1+\Gamma)$ and $\mathfrak{t}=2\Gamma/(1+\Gamma)$ are the reflection and transmission amplitudes of the 2/1 interface and

$$\Gamma_p=\frac{\varepsilon_1\overline{Q}_2}{\varepsilon_2\overline{Q}_1}, \tag{23}$$

$$\Gamma_s=\frac{\overline{Q}_1}{\overline{Q}_2}. \tag{24}$$

Equations (16)–(24) represent the complete solution. To clarify its content we now consider various special cases and limits. In these we shall assume $\beta^2\ll 1$, which allows us to set always $\overline{Q}_1=\overline{Q}_3\to Q=\sqrt{Q_y^2+Q_z^2}$. For the low-speed results that have been found before [6–9] we need to let $v\to 0$ in Eqs. (18)–(20). This leads one to consider how ε_2 behaves in the limit $\omega\to 0$. The conventional choice uses

$$\varepsilon_2=1+\frac{4\pi i\sigma_o}{\omega}, \tag{25}$$

where σ_o is the (finite) dc conductivity. The modifications of σ at higher frequencies have not been considered relevant, but of course could be included in numerical work. With the form (25) and $v\to 0$, one has $\overline{Q}_2\to Q$ and $\Gamma_s\to 1$ while $\Gamma_p\to 0$. Ignoring e_s compared to e_p, but keeping both b_s and b_p, we obtain the following low-speed formulas [10]

$$\vec{D}^{(0)}(\vec{x},t)=\int\frac{d^2Q}{(2\pi)^2}\vec{D}^{(0)}_{\text{total}}(x;\mathbf{Q})e^{iQ_y(y-vt)}e^{iQ_z z}, \tag{26}$$

with $\hat{x}\cdot\vec{D}^{(0)}_{\text{total}}$ given in the three regions $0<x$, $-d<x<0$, and $x<-d$, respectively, by

$$\hat{x}\cdot\vec{D}^{(0)}_{\text{total}}=-2\pi e\times\begin{cases}\text{sgn}(h-x)e^{-Q|x-h|}+e^{-Q(x+h)}\\ 2e^{-Qh}(e^{Qx}-e^{-Q(x+2d)})/(1-e^{-2Qd})\\ 0\end{cases} \tag{27}$$

and

$$\vec{B}^{(0)}(\vec{x},t)=\int\frac{d^2Q}{(2\pi)^2}\vec{B}^{(0)}_{\text{total}}(x;\mathbf{Q})e^{iQ_y(y-vt)}e^{iQ_z z}, \tag{28}$$

with $\hat{z}\cdot\vec{B}^{(0)}_{\text{total}}$ given in the three regions $0<x$, $-d<x<0$, $x<-d$, respectively, by

$$\hat{z}\cdot\vec{B}^{(0)}=2\pi e\beta\times\begin{cases}\text{sgn}(h-x)\quad e^{-Q|x-h|}+\dfrac{Q_y^2}{Q^2}e^{-Q(x+h)}\\ 2\dfrac{Q_y^2}{Q^2}e^{-Qh}(e^{Qx}-e^{-Q(x+2d)})/(1-e^{-2Qd})+\dfrac{Q_z^2}{Q^2}e^{-Q(h-x)}\\ \dfrac{Q_z^2}{Q^2}e^{-Q(h-x)}.\end{cases} \tag{29}$$

For simplicity we have written out explicitly here only a single field component.

Since $\varepsilon_2 \to \infty$, Eq. (27) shows that there is no $E_x^{(0)}$ for $x<0$ and no $D_x^{(0)}$ for $x<-d$. For $x>0$ we have the (static) image potential result. While only p waves make a significant contribution to $\vec{D}^{(0)}$ and $\vec{E}^{(0)}$, the magnetic field has important contributions from both polarizations. It is the s-wave part that allows $\vec{B}^{(0)}$ to extend beyond the slab. Note that in $x<-d$, $\vec{B}^{(0)}$ has no dependence on σ_o, d, or even the location of the conducting slab [8,9]. This remarkable behavior is explained in the optics language by saying that for $v \to 0$, the s waves suffer no reflection and the amplitude of the partial wave below $x=-d$ is set by $e^{-Qh}e^{-\overline{Q}_2 d}e^{Q(x+d)}$, which reduces to $e^{-Q(h-x)}$ since $\overline{Q}_2 \to Q$.

As an aside, note that for a perfect conductor one replaces Eq. (25) with $\varepsilon_2 = 1-(\omega_p^2/\omega^2)$, where ω_p is a plasma frequency. Then $\overline{Q}_2 \to (Q^2+1/\delta^2)^{1/2}$ with $\delta = c/\omega_p$, the frequency-independent penetration depth. In this case even the s waves will be (partially) reflected by the slab and the magnetic field on the far side will be attenuated by at least $e^{-d/\delta}$.

Coming back to the good, but not perfect, conductor case, it is of interest to compare the low-speed fields with the unscreened velocity fields. Setting $\varepsilon_2 = 1$, we have for all $\vec{x}$ when $\beta^2 \ll 1$,

$$\vec{D}^{(u)}(\vec{x},t) = 2\pi e \int \frac{d^2Q}{(2\pi)^2} e^{iQ_y(y-vt)} e^{iQ_z z} e^{-Q|x-h|} \times \left(-\mathrm{sgn}(h-x), -i\frac{Q_y}{Q}, -i\frac{Q_z}{Q} \right), \tag{30}$$

$$\vec{B}^{(u)}(\vec{x},t) = 2\pi e\beta \int \frac{d^2Q}{(2\pi)^2} e^{iQ_y(y-vt)} e^{iQ_z z} e^{-Q|x-h|} \times \left(-i\frac{Q_z}{Q}, 0, \mathrm{sgn}(h-x) \right). \tag{31}$$

If we specialize to $z=0$ and $y=vt$ (i.e., directly under the drifting charge), then at the top and below the bottom surface of the conductor we have [8]

$$D_x^{(0)}/D_x^{(u)} = \begin{cases} 2, & x=0 \\ 0, & x \leqslant -d, \end{cases} \tag{32}$$

$$B_z^{(0)}/B_z^{(u)} = \begin{cases} 3/2, & x=0 \\ 1/2, & x \leqslant -d, \end{cases} \tag{33}$$

The general x dependence is further discussed in Sec. III, but we emphasize here that for both $B^{(u)}$ and $B^{(0)}$ it is algebraic after the integrals over $\mathbf{Q}$.

Now consider how one moves out of the low-speed limit. This occurs in several ways, depending on which parameter is examined. For ε_2 we write

$$\varepsilon_2 = 1 + 2i\frac{v_{op}/v}{Q_y h} \tag{34}$$

with

$$v_{op} = 2\pi\sigma_o h, \tag{35}$$

while for $\overline{Q}_2$

$$\overline{Q}_2 = \left(Q^2 - 2i\frac{Q_y}{h}\frac{v}{v_{os}} \right)^{1/2} \tag{36}$$

with

$$v_{os} = \frac{c^2}{2\pi\sigma_o h}. \tag{37}$$

Since $v_{os}v_{op} = c^2$, one of these characteristic speeds will always be much greater than v. A typical value of $1/\sigma_o$ for a good conductor is 10 $\mu\Omega$ cm, which implies $2\pi\sigma_o \sim 6\times 10^{17}$/s. Then for most choices of h, $v_{op} \gg c$, and we need only be concerned with the relative size of v and v_{os}. To show in detail how $\vec{B}^{(0)}$ changes for $v \gtrsim v_{os}$ requires numerical work. However, Eq. (37) is useful for a qualitative estimate of when effects due to eddy currents and Lenz's law will become important [11].

Another set of limiting cases come from the variation of the slab thickness. For $d \to \infty$, we ignore α_- and t in Eq. (22) and replace

$$\alpha_+ \to \frac{2}{1+\Gamma}, \quad r \to \frac{\Gamma-1}{\Gamma+1}. \tag{38}$$

If we further let $v \to 0$, our results become equivalent to Boyer's, [7,10] but expressed in Fourier space. The limit $d \to 0$ is more subtle since we still want the metal to have an effect. One way to take the limit is to require $\overline{Q}_2 d \to 0$ and $\Gamma \to 0$. This occurs if we hold v fixed and let d and $1/\sigma_o$ become small. Then one needs to carefully expand the quantities in Eq. (22) as $\mathfrak{r}, e^{-\overline{Q}_2 d} \to 1$. The final results are controlled by the size of $\overline{Q}_2 d/\Gamma$ for which we find under these conditions

$$\overline{Q}_2 d/\Gamma_p \to 2i\frac{v_{1p}}{v}\frac{Q}{Q_y}, \quad v_{1p} = 2\pi\sigma_o d$$

$$\overline{Q}_2 d/\Gamma_s \to -2i\frac{v}{v_{1s}}\frac{Q_y}{Q}, \quad v_{1s} = c^2/2\pi\sigma_o d. \tag{39}$$

If v is small compared to both v_{1p} and v_{1s}, then $t_p \to 0$ and $t_s \to 1$ and our results reduce to those of Furry [8,11,12].

We end this section by examining various superpositions of our results. The fields we have calculated represent a linear response, so linear superposition should be justified and can be attempted in several ways. First consider charges moving along $\hat{y}$. In Eq. (12) replace $\delta(y-vt)$ with $\delta(y-y'-vt)$ and integrate over y'. Then

$$\frac{\lambda}{e}\int dy'\rho(\vec{x},t)=\lambda\,\delta(x-h)\,\delta(z)=\rho', \tag{40}$$

$$\frac{\lambda}{e}\int dy'\vec{j}(\vec{x},t)=\lambda v\hat{y}\,\delta(x-h)\,\delta(z)=\vec{j}'. \tag{41}$$

These new distributions represent a line of charge (with linear density λ) moving parallel to itself. There is no time dependence in either ρ' or $\vec{j}'$, so we expect separate electrostatic and magnetostatic solutions for $\vec{E}$ and $\vec{B}$. Applying the y' integration to our formal results depends on

$$\int_{-\infty}^{\infty}dy'\exp[iQ_y(y-y'-vt)]=2\pi\delta(Q_y), \tag{42}$$

which removes the time dependence and implies $\overline{Q_j}\to|Q_z|$, $\Gamma_p\to 0$, $\Gamma_s\to 1$. Incorporating these changes into Eqs. (16)–(22), we find

$$\vec{B}'(\vec{x},t)=2\pi\lambda\beta\int_{-\infty}^{\infty}\frac{dQ_z}{2\pi}e^{iQ_zz}\exp[-|Q_z||x-h|]$$
$$\times[-i\,\mathrm{sgn}(Q_z),0,\mathrm{sgn}(h-x)], \tag{43}$$

which is the static, unscreened $\vec{B}$ field due to line of current $I=v\lambda$ along $\hat{y}$. This may be confirmed by superposing via a y' integral the unscreened field of Eq. (31). The form of $\vec{D}'$ is more complicated because the electrostatic field is screened. The results follow from inserting $2\pi\delta(Q_y)\lambda/e$ into the integrand of Eq. (26).

We also can build a line of charge by replacing in Eqs. (1) and (2) $\delta(z)$ with $\delta(z-z'')$ and integrating over z''. Then

$$\frac{\lambda}{e}\int dz''\rho(\vec{x},t)=\lambda\,\delta(x-h)\,\delta(y-vt), \tag{44}$$

$$\frac{\lambda}{e}\int dz''\vec{j}(\vec{x},t)=\lambda v\hat{y}\,\delta(x-h)\,\delta(y-vt), \tag{45}$$

which are the distributions for a line of charge moving perpendicular to itself. Note that a time dependence remains in Eqs. (44) and (45). In the low-speed limit, $\vec{D}''$ due to Eqs. (44) and (45) agrees with $\vec{D}'$ due to Eqs. (40) and (41), aside from a change of axis labels. However $\vec{B}''$ is quite different from $\vec{B}'$. One needs to insert $2\pi\delta(Q_z)\lambda/e$ into Eq. (19), or in the low-speed limit into Eq. (28). Using the latter, we find $B_z''=-\beta D_x''$ so the magnetic field is screened just as efficiently as the displacement field. This occurs because both are here carried only by *p*-waves. We also remark that B_z'' appears to agree with Jones' general result [2]. One needs to replace our Q_y with ω/v, let $d\to\infty$, and identify his $-\alpha$ with our Γ_p+1.

It is not unreasonable that $\vec{B}'$ and $\vec{B}''$ differ so much since the motions of the lines of charge in Eqs. (41) and (45) are quite distinct. More perplexing puzzles arise if we try a further superposition of line charges to create a drifting charge sheet. This could be done either by integrating Eqs. (40) and (41) over z', or by integrating Eqs. (44) and (45) over y'. The final source distribution would be the same in both cases: a uniform charge sheet at height h drifting at velocity $v\hat{y}$. However such a double superposition of the magnetic fields we have found depends on whether the y' or z' integral is done first [7]. The mathematical origin of the ambiguity can be seen in Eq. (29), where factors of Q_y^2/Q^2 and Q_z^2/Q^2 appear. These do not have a unique limit as $\mathbf{Q}\to\mathbf{0}$. One needs to know whether Q_y or Q_z goes to zero first. We do not see a clear way to resolve this ambiguity. One probably needs to worry as $\mathbf{Q}\to\mathbf{0}$ about charges and/or currents at infinity (in the y-z plane). Note that similar puzzles can arise when one tries to integrate the B field over both z and t [13], since for a constant speed $\int dt'\sim\int dy'/v$.

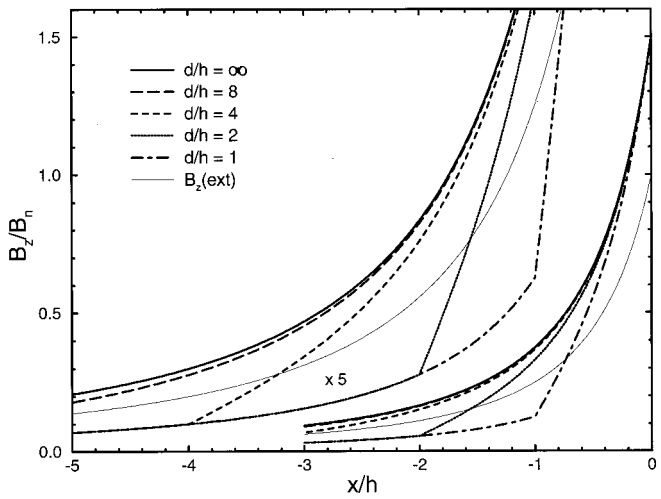

FIG. 1. The z component of the magnetic field directly under the drifting charge versus depth into and below the conducting slab. The various thick lines show the low-speed approximation $B_z^{(0)}$ for different choices of slab thickness, while the single thin line is the unscreened $B_z^{(u)}=B_z(\mathrm{ext})$. All the curves are normalized to $B_n=\beta e/h^2$, and the data on the left side have been multiplied by a factor of 5.

III. MODEL CALCULATIONS

So far our analysis has usually left the **Q** integrals implicit. The integrals can be done explicitly for both the unscreened and low-speed limits; see Refs. [6–9] for their form. For arbitrary speed v analytic integration does not seem to be possible so we turn to numerical calculations, focusing on $B_z(x,y,z=0,t)$.

Begin with an interpolation between the values noted in Eq. (33). For $y=vt$, $z=0$, and $x<h$, $B_z^{(u)}=\beta e/(h-x)^2$ and $B_z^{(0)}$ may be computed from Eq. (29). In Fig. 1 we compare these two results versus x at fixed h for several choices of d. Consistent with Eq. (33), $B_z^{(0)}$ falls from larger to smaller than $B_z^{(u)}$ as one moves from the top to the bottom of the conducting slab. Below $x=-d$, $B_z^{(0)}=\frac{1}{2}B_z^{(u)}$. For $d\to\infty$, $B_z^{(0)}=\frac{3}{2}B_z^{(u)}$ throughout the conductor (along the line $y=vt$, $z=0$). These results depend on β only through the prefactor and are independent of σ_o. They represent the

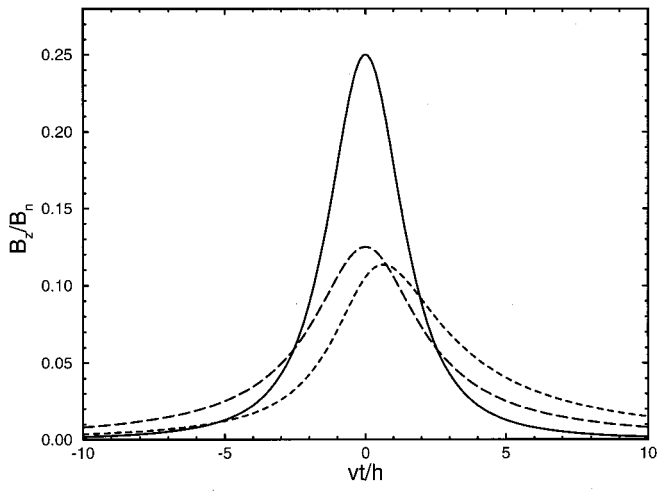

FIG. 2. The z component of the magnetic field at a fixed location versus time. The solid curve is the unscreened result; the long-dashed curve the low-speed result; and the short-dashed curve the general result with $v/v_{os}=2$ and $v_{os}/c=10^{-4}$. The observation point is on the bottom of a slab of thickness $d=h$. All the curves are normalized to $B_n=\beta e/h^2$.

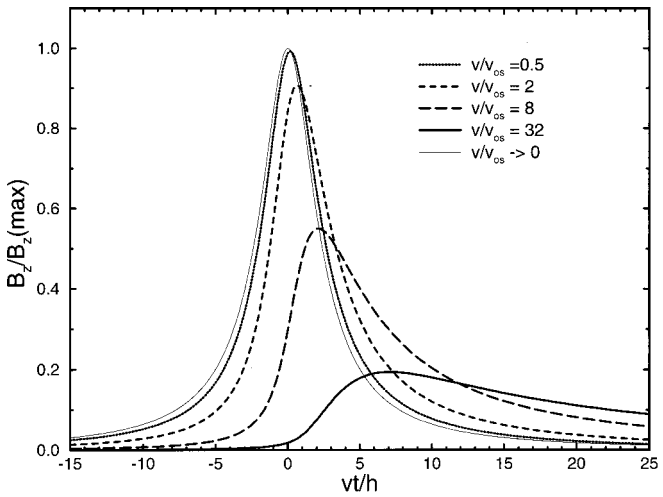

FIG. 3. The z component of the magnetic field at the same observation point as in Fig. 2 versus time. The different thick curves are labeled by the values of v/v_{os} with $v_{os}/c=10^{-4}$. The single thin line is the low-speed result $B_z^{(0)}$. Its maximum value is used to normalize all the curves.

maximum value that B_z can reach for $vt\neq y$, if $\beta^2\ll 1$.

In Fig. 2 this last point is illustrated by plotting B_z for fixed $x=-d$, $y=0$, $z=0$ versus vt. At $t=0$ the charge is directly above the observation point. Note that the unscreened and low-speed fields are symmetric functions of t. For large $|t|$ the former decays as $|t|^{-3}$, while the latter decays as $|t|^{-2}$. The new result is the asymmetric curve with $v/v_{os}=2$. Note that the general B_z rises and falls more slowly than $B_z^{(0)}$ and that its maximum value is less.

A remarkable property of all the results is that $\int_{-\infty}^{\infty}dt\,B_z(\vec{x},t)$ is invariant; i.e., the area under each of the curves in Fig. 2 is the same [1]. To understand this note that

$$\int_{-\infty}^{\infty}dt\vec{B}(\vec{x},t)=\vec{B}(\vec{x},\omega=0). \tag{46}$$

The field at zero frequency is determined by the sources at zero frequency. Going back to Eqs. (1) and (2) we have

$$\rho(\vec{x},\omega=0)=\frac{e}{v}\delta(x-h)\,\delta(z), \tag{47}$$

$$\vec{j}(\vec{x},\omega=0)=e\hat{y}\,\delta(x-h)\,\delta(z). \tag{48}$$

The response to these sources is determined by separate electrostatic and magnetostatic calculations. For $\vec{B}(\vec{x},\omega=0)$, the source $\vec{j}$ is a dc line current. Since at $\omega=0$ the magnetic field is unaffected by any (except perfect) conductor — see Eq. (10) — we deduce that $\vec{B}(\vec{x},\omega=0)$ is independent of v, and given by its unscreened value

$$\vec{B}(\vec{x},\omega=0)=\frac{2e}{c}\,\frac{(z,0,h-x)}{(h-x)^2+z^2}. \tag{49}$$

We used this invariant as a check on our numerical accuracy.

To more fully show how the general result evolves away from the low-speed limit, we present in Fig. 3 results for a range of v/v_{os} values. There is a smooth qualitative trend in the shape of the curves, but the integrated area under each is the same. We have also examined similar sets of curves for different, fixed observation points. For x placed further below the charge's path, the sensitivity to v/v_{os} increases. In the other direction, say when the observation point is on the top face of the conductor, both $B_z^{(0)}$ and B_z have extended regions of negative values, before rising quickly to values larger than the always positive $B_z^{(u)}$. For increasing v/v_{os} the negative values of B_z for $t<0$ move toward positive values while the negative values for $t>0$ become even more negative and longer ranged.

To summarize we have shown in this paper how to obtain a full solution to a simple electromagnetism problem. Our solution requires no limitations on the speed of the drifting charge. Although the characteristic speeds $v_{os}, v_{op}, v_{1s}, v_{1p}$ have long been known to be relevant, [6,11,14] ours is the first theory that allows explicit calculations to be done for v exceeding some of these. It remains for future work to determine whether the results found here can help resolve the controversy about a possible classical explanation of the Bohm-Aharonov effect [1].

ACKNOWLEDGMENTS

We are grateful to Professor Timothy Boyer for helpful correspondence. Part of the calculations were done on the Cray Research Inc. T90 system at NPACI, San Diego, California.

[1] T.H. Boyer, Am. J. Phys. **67**, 954 (1999).
[2] D.S. Jones, J. Phys. A **8**, 742 (1975).
[3] J. D. Jackson, *Classical Electrodynamics* (Wiley, New York, 1975).
[4] The real part of $\varepsilon(\omega)$ may have either sign, but we assume that the imaginary part has the same sign as ω.
[5] M. Born and E. Wolf, *Principles of Optics* (Pergamon Press, New York, 1959).
[6] J.S. Shier, Am. J. Phys. **36**, 245 (1968).
[7] T.H. Boyer, Phys. Rev. A **9**, 68 (1974).
[8] W.H. Furry, Am. J. Phys. **42**, 649 (1974).
[9] T.H. Boyer, Phys. Rev. E **53**, 6450 (1996).
[10] The earlier works [6–9] in effect do set $\overline{Q_2}=Q$ so $\Gamma_s=1$, but use $\Gamma_p=1/\varepsilon_2\approx -iv Q_y/(4\pi\sigma_o)$, which produces a small correction to Eq. (27). See discussion below Eqs. (34)–(37).
[11] W.M. Saslow, Am. J. Phys. **60**, 693 (1992).
[12] We caution that Furry's meaning for ''perfect conductor'' differs from ours.
[13] T.H. Boyer, Found. Phys. **30**, 893 (2000).
[14] E. Kasper, Optik (Stuttgart) **42**, 367 (1975).